

Title

The gene *paaZ* of the phenylacetic acid (PAA) catabolic pathway branching point and *ech* outside the PAA catabolon gene cluster are synergistically involved in the biosynthesis of the iron scavenger 7-Hydroxytropolone in *Pseudomonas donghuensis* HYS.

Panning Wang, Yaqian Xiao, Donghao Gao, Yan Long * and Zhixiong Xie *

Hubei Key Laboratory of Cell Homeostasis, College of Life Sciences, Wuhan University, Wuhan 430072, China;

2015202040019@whu.edu.cn (P.W.); 2018102040012@whu.edu.cn (Y.X.);

2021202040036@whu.edu.cn (D.G.);

* Correspondence: skyjck4@whu.edu.cn (Y.L.); zxxie@whu.edu.cn (Z.X.)

Supplemental Materials

Screening and characterization of transposon mutants with reduced siderophore production.

As identified in our previous work [20, 22], to define the essential genes involved in the biosynthesis of siderophores, random transposon insertion mutation was carried out using the vector pBT20 and modified chromeazurol S (CAS) agar assays in *P. donghuensis* HYS. The mutants deficient in siderophore yields were obtained in *P. donghuensis* HYS. Then, sequence alignment of the transposon-flanking sequences of the insertion sites in these 9 mutants with the genome sequence of *P. donghuensis* HYS indicated that the mutant genes were mainly located on cluster 2 (Table S1 and Figure 1A).

These 9 mutant strains were inserted in 5 different genes in cluster 2 (Table S1 and Figure. 1A). Six of these mutants (M7, M54, M1, M37, M49, M50) showed insertions in five ORFs (*orf17*, *orf19–orf21*) may arrange sequentially in the genome, and the other three mutants (M31, M40, M60) inserted in the *orf26*. The siderophores production of the 9 mutant strains was significantly lower than that of the wild-type HYS, suggesting that the genes *orf17*, *orf19–orf21*, and *orf26* corresponding to the 9 mutant strains were related to the biosynthesis of siderophores in *P. donghuensis* HYS.

Table S1. Characteristics of the 9 transposon mutants of *P. donghuensis* HYS.

Mutant ^a	Insertion site ^b	Insertion gene function ^c	Relative siderophore production ^d	
			CAS plate	Liquid medium
M7	Scaffold18 84439-84440	Phenylacetic acid degradation protein	0.18 ± 0.01	0.17 ± 0.01
M54	Scaffold18 84549-84550	Phenylacetic acid degradation protein	0.15 ± 0.01	0.16 ± 0.00
M1	Scaffold18 86359-86360	Phenylacetic acid degradation protein	0.14 ± 0.00	0.16 ± 0.00
M37	Scaffold18 86766-86767	Phenylacetate-CoA oxygenase	0.18 ± 0.01	0.15 ± 0.00
M49	Scaffold18 87193-87194	Phenylacetate-CoA oxygenase subunit PaaA	0.12 ± 0.00	0.16 ± 0.00
M50	Scaffold18 88042-88043	Phenylacetate-CoA oxygenase subunit PaaA	0.15 ± 0.02	0.16 ± 0.01
M60	Scaffold18 92847-92848	Enoyl-CoA hydratase	0.20 ± 0.00	0.15 ± 0.00
M40	Scaffold18 93134-93135	Enoyl-CoA hydratase	0.16 ± 0.01	0.15 ± 0.00
M31	Scaffold18 93315-93316	Enoyl-CoA hydratase	0.15 ± 0.02	0.16 ± 0.00

^aThe mutant strains are displayed according to their relative positions on the scaffold of the HYS genome.

^bThe insertion site is located between the two bases shown.

^cThe possible functions of genes are based on genomic annotation of *P. donghuensis* HYS.

^dThe relative ferrider-producing capacity was the ratio of ferrider-producing capacity of mutant strain to ferrider-producing capacity of wild-type HYS. On the CAS test plate, the siderophore production capacity was the radius value of the chelated halos; In MKB liquid medium, it is the number of siderophore units (%) produced by bacteria per OD₆₀₀ (see Materials and methods for details). Each value is the mean ± standard deviation of at least three independent experiments.

Table S2. Characteristics of genes in cluster 2 in *P. donghuensis* HYS.

Gene	No.of amino acid residues	Proposed Function(s) ^a	Organism	% identity ^b	% coverage	Significance (E value)	Accession no.
<i>orf13</i>	689	Phenylacetic acid degradation bifunctional protein PaaZ	<i>E.coli</i> K-12	57.8	98	0.0	THI66261.1
<i>orf14</i>	413	OprD family outer membrane porin	<i>E.coli</i> M34	80.87	100	0.0	MRF40643.1
<i>orf15</i>	513	Cation/acetate symporter ActP	<i>E.coli</i> K-12	69.6	100	0.0	HBP1329774.1
<i>orf16</i>	102	DUF485 family inner membrane protein	<i>E.coli</i> K-12	42.1	92	1e-21	HBP1325669.1
<i>orf17</i>	358	Phenylacetate-CoA oxygenase/reductase subunit PaaE	<i>E.coli</i> K-12	50.0	99	3e-119	THH46419.1
<i>orf18</i>	177	Phenylacetate-CoA oxygenase/reductase subunit PaaD	<i>E.coli</i> K-12	53.3	86	4e-53	THI66257.1
<i>orf19</i>	251	Phenylacetate-CoA oxygenase/reductase subunit PaaC	<i>E.coli</i> K-12	51.0	98	4e-87	THI66258.1
<i>orf20</i>	93	Phenylacetate-CoA oxygenase/reductase subunit PaaB	<i>E.coli</i> K-12	58.9	96	1e-38	NP_415907.1
<i>orf21</i>	329	Phenylacetate-CoA oxygenase/reductase subunit PaaA	<i>E.coli</i> K-12	68.0	93	2e-164	NP_415906.1
<i>orf22</i>	436	Phenylacetate—CoA ligase PaaK	<i>E.coli</i> K-12	68.2	97	0.0	THI66250.1
<i>orf23</i>	403	3-oxoadipyl-CoA thiolase PaaJ	<i>E.coli</i> K-12	70.3	99	0.0	NP_415915.1
<i>orf24</i>	142	Hydroxyphenylacetyl-CoA thioesterase PaaI	<i>E.coli</i> K-12	44.4	95	1e-37	THI66252.1
<i>orf25</i>	505	3-hydroxyacyl-CoA dehydrogenase PaaH	<i>E.coli</i> K-12	47.1	96	1e-134	NP_415913.1
<i>orf26</i>	263	2-(1,2-epoxy-1,2-dihydrophenyl)acetyl-CoA isomerase	<i>E.coli</i> K-12	62.8	99	4e-109	THH46417.1
<i>orf27</i>	256	2,3-dehydroadipyl-CoA hydratase	<i>E.coli</i> K-12	57.9	98	2e-96	NP_415911.1
<i>orf28</i>	198	Phenylacetic acid degradation protein PaaY	<i>E.coli</i> K-12	58.5	97	5e-80	THI66248.1
<i>orf29</i>	307	Phenylacetic acid degradation operon negative regulatory protein PaaX	<i>E.coli</i> K-12	43.6	99	2e-87	THH46412.1

^aCoA, coenzyme A.

^bSimilarity values are for the most similar proteins, determined by BLASTP analysis, whose functions and source organisms are also shown.

Analysis and identification of transcriptional units and promoters of cluster 2.

In order to further determine the relationship between the genes *orf17*, *orf19–orf21*, *orf26* screened by transposon insertion mutation in cluster 2 and the biosynthesis of siderophore, we analyzed and identified the transcriptional units of these genes. *orf17–orf21* are arranged in a 5 kb region of the HYS genome, which have the same transcription direction as the downstream genes *orf14–orf16* and the upstream genes *orf22–orf27* (Figure 1A). In addition, the distance between adjacent gene sequences was close or partially overlapped, so we speculated that there may be co-transcriptional relationships between them.

Firstly, to search for and analyze potential promoters in this region, we use a promoter prediction program (http://www.fruitfly.org/seq_tools/promoter.html), and found possible promoters in front of *orf21* and *orf27* respectively (Minimum promoter score=0.8) (data not shown).

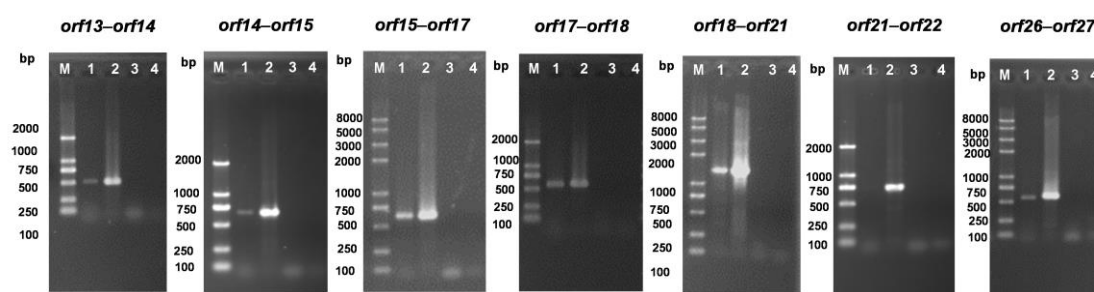


Figure S1. RT-PCR of RNA extracted from *P. donghuensis* HYS with ORF connecting primer pairs (*orf13–orf14* RT-1 plus *orf13–orf14* RT-2, *orf14–orf15* RT-1 plus *orf14–orf15* RT-2, *orf15–orf17* RT-1 plus *orf15–orf17* RT-2, *orf17–orf18* RT-1 plus *orf17–orf18* RT-2, *orf18–orf21* RT-1 plus *orf18–orf21* RT-2, *orf21–orf22* RT-1 plus *orf21–orf22* RT-2, *orf26–orf27* RT-1 plus *orf26–orf27* RT-2). The different lanes represent different templates: lanes M, DNA Maker; lane 1, cDNA; lane 2, genomic DNA as a positive control; lane 3, RNA without reverse transcription as a negative control; lane 4, ddH₂O as a blank control.

Furthermore, to confirm the transcriptional relationships among these genes, primer pairs (Table.S5) connecting neighboring (intergenic region) ORFs were used to do the Reverse transcription (RT-PCR). The results showed that products generated using HYS cDNA as the template were similar to those obtained using genomic DNA as the template for these (*orf13–orf14*, *orf14–orf15*, *orf15–orf17*, *orf17–orf18*, *orf18–orf21*, *orf21–orf22*, *orf26–orf27*) connecting primer pairs, in addition to the *orf21–22* connecting primer pairs without target products formed using HYS cDNA as the template (Figure S1). The negative and blank control using genome-removed RNA and ddH₂O as the template respectively did not produce the target bands. The target fragments amplified by genomic cDNA as template were extracted and sequenced, and the sequencing results were all correct, which were the corresponding cross-gene target sequences. The above Reverse transcription PCRs results indicated that there was a co-transcriptional relationships of *orf13–orf21*, and the cotranscription of *orf26–orf27*, but

no co-transcriptional relationships between *orf21* and *orf22*. According to the promoter prediction and co-transcriptional analysis results, the predicted promoter in front of *orf21* was used for further studies on *orf17–orf21* and the predicted promoter upstream of *orf27* was used for further studies on *orf26*.

Detection of the phenylacetic acid metabolic ability of related genes on gene cluster 2 by using phenylacetic acid as a single carbon source.

The arrangement and annotation of cluster 2 were shown in Figure.1A. Through NCBI BLASTP analysis, proteins encoded by genes in cluster 2 shared high similarity (43–70%) with proteins encoded by genes in PAA cluster genes of *E.coli* K-12 (Table S2), suggesting that cluster 2 may be a phenylacetic acid metabolic cluster.

To investigate whether 7-HT related genes in cluster 2 were involved in phenylacetic acid metabolism, phenylacetic acid was added to the M9 minimal medium as a sole carbon source. In the experiment, it was found that HYS, $\Delta orf13$ ($\Delta paaZ$), $\Delta orf17$ ($\Delta paaE$), $\Delta orf18$ ($\Delta paaD$), $\Delta orf19$ ($\Delta paaC$), $\Delta orf20$ ($\Delta paaB$), $\Delta orf21$ ($\Delta paaA$), $\Delta orf26$ ($\Delta paaG$), $\Delta orf17–21$ ($\Delta paaEDCBA$) and $\Delta orf26$ ($\Delta paaG$) strains were cultured in M9 medium with 0.4% glucose (Glu) as a single carbon source to the stationary phase, compared with the wild-type HYS, each knockout strain had no obvious growth difference, indicating that the knockout of these genes did not affect the glucose utilization of *P. donghuensis* HYS (Figure S2A). When phenylacetic acid was used as the sole carbon source for cultivation to the stationary phase, compared with the wild-type strain HYS, the knockout strains $\Delta orf13$ ($\Delta paaZ$), $\Delta orf17$ ($\Delta paaE$), $\Delta orf18$ ($\Delta paaD$), $\Delta orf19$ ($\Delta paaC$), $\Delta orf20$ ($\Delta paaB$), $\Delta orf21$ ($\Delta paaA$), $\Delta orf26$ ($\Delta paaG$), $\Delta orf17–21$ ($\Delta paaEDCBA$) could not grow (FigureS 2B), indicating that these deletion strains cannot utilize phenylacetic acid. The knockout strains $\Delta orf17$ ($\Delta paaE$), $\Delta orf18$ ($\Delta paaD$), $\Delta orf19$ ($\Delta paaC$), $\Delta orf20$ ($\Delta paaB$), $\Delta orf21$ ($\Delta paaA$), $\Delta orf26$ ($\Delta paaG$), $\Delta orf17–21$ ($\Delta paaEDCBA$) exhibited significant growth deficiency when phenylacetic acid was used as sole carbon source (Figure S2 B).

In summary, the sole carbon utilization experiments showed that the knockout of *orf13*, *orf17–21*, and *orf26* genes in gene cluster 2 caused the strain unable to use phenylacetic acid for growth, so it was preliminarily clarified that these genes in cluster 2 were involved in the catabolism of phenylacetic acid in *P. donghuensis* HYS. Moreover, the phenylacetic acid degradation pathway is involved in the biosynthesis of 7-HT in *P. donghuensis* HYS (Figure 1), which provides a direction for the study of the 7-HT biosynthesis pathway.

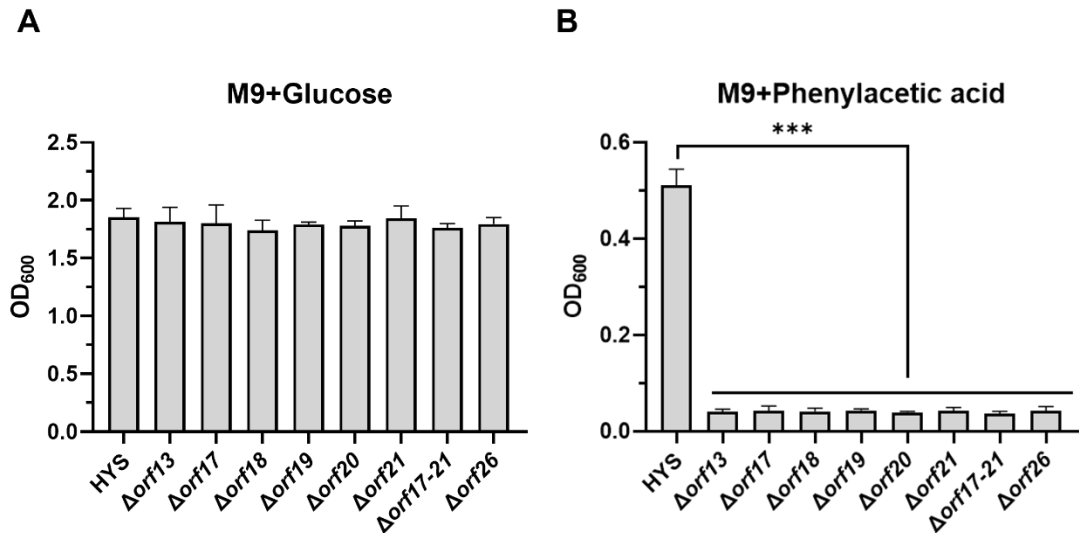


Figure S2. Growth of wild-type HYS and each knockout strain in a single carbon source at the stationary phase. (A) M9 minimal medium with 0.4% glucose as a single carbon source. (B) M9 minimal medium with 0.6 mg/ml phenylacetic acid as a single carbon source. Each value is the average from three different cultures \pm the standard deviation. OD₆₀₀, optical density at 600 nm. *** $p < 0.001$, Student's t -test.

Table S3. Characteristics of Paaz-ECH homologous protein^a in *P. donghuensis* HYS

Description	Scientific Name	Max Score	Total Score	Query Cover	E value	Per. Ident	Acc Len	Accession ^b
(R)-hydratase [(R)-specific enoyl-CoA hydratase]	<i>P. donghuensis</i> HYS	63.5	63.5	90%	1×10^{-13}	32.45%	156	UW3_RS0113785
NodN (nodulation factor N)	<i>P. donghuensis</i> HYS	54.7	54.7	50%	2×10^{-10}	32.18	151	UW3_RS0112810

^aSimilarity values are for the most similar protein, determined by BLASTP analysis.

^bGene id in *P. donghuensis* HYS.

Alignment Scores <40 40–50 50–80 80–200 ≥200

Distribution of the top 2 Blast Hits on 2 subject sequences

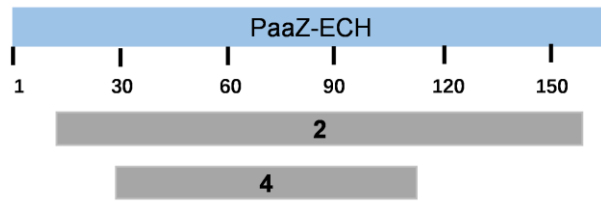


Figure S3. Distribution of the 2 proteins (ECH and NodN) with homology to the C-terminal ECH domain of ORF13 (PaaZ) obtained by whole genome alignment search of *P. donghuensis* HYS.

EGV41540	TNRVTRAEVEAGTAEHPFRKDLATLKGIDCFASELREVIMGEIQFAEETGDTFFYAEVNEEAAAMRNPEFP	70
NP_415905AKVEEDR..IHPFRKYFEELQFGDSLLTFRRTMTEADIVNFAQLSGDHFYAEAMKIRAAES.IFG	62
NP_745413GEVIETE..VHPFRRYFEQLRVGESSLLTHRRVTVEADLVNFGQLSGDHFYAEFTEIRAKAS.CFG	62
NP_947071AFAPAAE..VHPFKLNYNQLEIQGSIETASFPITLDEIEFAHFTGDTFFYAEVNEEAAKANPEFP	63
YP_001105742GRSVID...VHPFRKHLEDLRVGDIVMAGFRAVILEUVEFAEFTGDTFFYAEVNEEAAKANPEFP	62
YP_001335130ACVNEDR..IHPFRKYFEELQFGDSLLTFRRTMTEADIVNFAQLSGDHFYAEAMKIRAAES.IFG	62
YP_001542038ATETPAP..AHPFTRGFADLRIGETLHTAFARQVILADIEFAAFTGDTFFYAEVMDAAAARNPEFP	63
YP_612432GPETIGP..AHPFTRRFGALTIGETLHTAFVWVTSDEVAFAAFTGDTFFYAEVMDAAAARNPEFP	63
WP_007118518AQEITDR..DHPFTRRETELDELGETFFYKSRREISLDDIETAFANFTGDTFFYAEVMDAAAARNPEFP	63
WP_009073845GFRVEG...EHPFRKSLAELSIGDITVAGFRTVTRADIDFAEFTGDTFFYAEVTEAAAAANPLFG	62
YP_006574071GTEIAAK..VHPFTRKFGDELGETLHSAARQITLEDIETFAHFTGDTFFYAEVMDAAAARNPEFP	63
YP_006575081AETRHN..GHPFRKSLLETLRIGDQLITETPQITEQVECEFAHFTGDTFFYAEVMDAAAARNPEFP	62
CAI08632.1MSEAVRDFSCQGHDFEDLKVMSAAIG.RIVTEADIAIFAGISGDTNPFVLLDAEFAAST.MFG	62
UW3_RS0120680AEVIETE..VHPFRRYFQDLRIGESSLLTHRRVTVEADLVNFGQLSGDHFYAEFTEIRARDS.CFG	62
UW3_RS0113785VMTQVINTPVEALEVCGTASFS.KTVEERLIQIFRAMSGDHNPFVLLDAEFAAKS.MFK	56
	g f g d h a f	
	39 44	
EGV41540	RRVHCGYLLVSWAAGLFVPEAGGPPVLANYGLENLRFICQPVTYGDSIRVELTAKRITER....VIDEYGE	135
NP_415905	ERVVHGYFVLSAAAGLFVDAGVGPVIANYGLESLEFIEPVKFGDITICVRLTCRRKILKKQRSAAEKPTGV	132
NP_745413	KRIHCGYFVLSAAAGLFVSPGGPVLANYGLDILRFINFPVIGDITICARLTCKRRIKIDGQKTSPLGQPCQV	132
NP_947071	GRVHCGYLLVSWAAGLFVPEAGGPPVLANYGLENLRFELKPVSPDSSIKVRLTVKQKSPA....RRFEYGE	128
YP_001105742	GRVHCGYLLVSWAAGLFVPEAGGPPVLANYGLENLRFITETTYFGDELTVLTAQCITER....VNAEHGE	127
YP_001335130	ERVVHGYFVLSAAAGLFVDAGVGPVIANYGLENLRFIEFVKFGDITICVRLTCRRKTVKRQRSADKATGV	132
YP_001542038	GRVHCGYLLVSWAAGLFVPEAGGPPVLANYGLDLSLRFKPVAFGDSIKARLTVKHKTP....RNDAYGE	127
YP_612432	GRVHCGYLLVSWAAGLFVPEAGGPPVLANYGLDNLRFEMKPVSPDSSIKVRLTVKAKTP....RNEYGE	127
WP_007118518	GRVHCGYLLVSWAAGLFVPEAGGPPVLANYGLDNLRFLEFVSAGDSMKVRLTVKHKTP....RNEEYGE	127
WP_009073845	GIVHCGYLLVSWAAGLFVSPGGPVLANYGLENLRFITVVKVDDQLTVLTAQCITER....IDQEYGE	127
YP_006574071	GRVHCGYLLVSWAAGLFVPEAGGPPVLANYGLDNLRFEMKPVSPDSSIKVRLTVKHKTP....RNEDYEQ	127
YP_006575081	DRVHCGYLLVSWAAGLFVPEAGGPPVLANYGLDNLRFHAEVYFGDCLHVRVTCREITER....ASAPFGD	127
CAI08632.1	ERIRHGMFLSASFISAVVGTGKLEGGCIYIC.QSINFKASVVKVGETVVARVTVRELVA....HKR	121
UW3_RS0120680	KRIHCGYFVLSAAAGLFVSAAGGPPVLANYGLDILRFINFPVIGDITICARLTCKRRIKIDGQKSPQGPQV	132
UW3_RS0113785	ERIRHGMFLSAGLISAAVACELEGGGTIYIC.QTMSFQKPVKFGDTLTVRLEILEKLE.....KFK	115
	h g p g f	
	62	
EGV41540	VANDTVLYNQDDEIVAAVDVLLIVLVEKVNTTYANDCKAEELAGV.....	178
NP_415905	VENAVEVFNCHQTPVALYSILTLVVRQHGDFVD.....	165
NP_745413	VANDVEVTNQLGELVVSNDILTLVLKKA.....	161
NP_947071	VRWDVEVVNQNGEFVARVDLLTMSARPA.....	157
YP_001105742	VRWDADVTNCGVESVAKYDVLTLVAKRPEEKA.....	159
YP_001335130	VENAVEIFNCHQCAVALYSILTLVVRQGGDFRRDSEK.....	169
YP_001542038	VRWHVSLTNQEDDLVAEYELLTMIAYAA.....	155
YP_612432	VRWHVSLTNQDDELVAEYDLLTMVAF.....	153
WP_007118518	VRWHVSLTNQREEAVVYDILLTMNAL.....	153
WP_009073845	VRWDADVTNCGDGSVAKYDVLTLVLSKEQP.....	156
YP_006574071	VRWHVSLTNQDDEIAAEYELLTMNAF.....	153
YP_006575081	VRWDCCVLLNACGVVVRREDLLTLVVKRSPVPPQDNVSEHKAAFPHTAATPHRAQDFVQQPA	187
CAI08632.1	RAEFDTVCTVAGKVVLLEGHAEIYLPARQ.....	149
UW3_RS0120680	VANDVEVTNQLGELVVSNDILTLVVKREVSFVAT.....	166
UW3_RS0113785	VRIRATRVFNQNDLNVVDGEAEILAPRKQQTVDLVSPFFITIG.....	157

Figure S4 Partial sequence alignment of PaaZ-ECH domain of a selection PaaZ orthologues with ECH and highlight the selected residues and conserved consensus sequence. Protein sequences for alignment from a selection of bacteria (EGV41540:*Corynebacterium glutamicum*, NP_415905: *Escherichia coli*, NP_745413:*Pseudomonas putida*, NP_947071:*Rhodopseudomonas palustris*, YP_001105742:*Saccharopolyspora erythraea*, YP_001335130: *Klebsiella pneumoniae*, YP_001542038: *Dinoroseobacter shibae*, YP_612432: *Ruegeria sp.*, WP_007118518: *Oceanibulbus indolifex*, WP_009073845: *Streptomyces sp.*, YP_006574071: *Phaeobacter inhibens* PaaZ1, YP_006575081: *Phaeobacter inhibens* PaaZ2, CAI08632.1: *Aromatoleum aromaticum* ECH-Aa, UW3_RS0120680: *P. donghuensis* HYS PaaZ, UW3_RS0113785: *P. donghuensis* HYS ech. Inside the red rectangle is the ECH-like conserved consensus sequence of ECH of *P. donghuensis* HYS. The red squares indicate the assumed key conserved residues (D-39, H-44, G-62) of the ECH domain in *P. donghuensis* HYS, each residue was mutated into Alanine by site mutation. Consistent residues (D, H, G) of *E. coli* PaaZ-ECH have been identified. The number indicates the position of the residue in the sequence of the ECH domain.

Table S4 Bacterial strains and plasmids used in this study

Strain or plasmid	Description ^a	Source or reference(s)
<i>E. coli</i> S17-1 λpir	<i>thi pro hsdR recA</i> ; chromosomal RP4-2; (Tc::Mu) (Km::Tn7) T _p ^r Sp ^r	[47]
<i>Pseudomonas</i> strains		
HYS	Wild-type <i>P. donghuensis</i> HYS ^T ; Cm ^r	[18,19,20]
Δorf17	<i>paaE</i> deletion strain	This study
Δorf18	<i>paaD</i> deletion strain	This study
Δorf19	<i>paaC</i> deletion strain	This study
Δorf20	<i>paaB</i> deletion strain	This study
Δorf21	<i>paaA</i> deletion strain	This study
Δorf17–21	<i>paaEDCBA</i> deletion strain	This study
Δorf26	<i>paaG</i> deletion strain	This study
Δorf13 (<i>paaZ</i>)	<i>paaZ</i> deletion strain	This study
Δech	<i>ech</i> deletion strain	This study
ΔNodN	<i>NodN</i> deletion	This study

<i>ΔpaaZΔech</i>	<i>paaZ</i> , <i>ech</i> deletion strain	This study
<i>Δech/pBBR2</i>	<i>Δech</i> complemented with pBBR1MCS-2	This study
<i>ΔpaaZΔech/pBBR2</i>	<i>ΔpaaZΔech</i> complemented with pBBR1MCS-2	This study
<i>Δech/pBBR2-ech</i>	<i>Δech</i> complemented with pBBR2- <i>ech</i>	This study
<i>ΔpaaZΔech/pBBR2-ech</i>	<i>ΔpaaZΔech</i> complemented with pBBR2- <i>ech</i>	This study
<i>Δech/pBBR2-echD39A</i>	<i>Δech</i> complemented with pBBR2- <i>echD39A</i>	This study
<i>Δech/pBBR2-echH44A</i>	<i>Δech</i> complemented with pBBR2- <i>echH44A</i>	This study
<i>Δech/pBBR2-echG62A</i>	<i>Δech</i> complemented with pBBR2- <i>echG62A</i>	This study
<i>Δech/pBBR2-paaZ</i>	<i>Δech</i> complemented with pBBR2- <i>paaZ</i>	This study
<i>Δech/pBBR2-paaZE258Q</i>	<i>Δech</i> complemented with pBBR2- <i>paaZE258Q</i>	This study
HYS/pBBR2	HYS complemented with pBBR1MCS-2	This study
HYS/pBBR2- <i>paaZ</i>	HYS complemented with pBBR2- <i>paaZ</i>	This study
HYS/pBBR2- <i>paaZE258Q</i>	HYS complemented with pBBR2- <i>paaZE258Q</i>	This study
Plasmids		
pEX18Gm	Gene replacement vector with MCS from pUC18; Gm ^r <i>oriT sacB</i>	[48]
pEX18Gm- <i>orf17</i> -UD	Gene replacement vector for <i>orf17</i>	This study
pEX18Gm- <i>orf18</i> -UD	Gene replacement vector for <i>orf18</i>	This study
pEX18Gm- <i>orf19</i> -UD	Gene replacement vector for <i>orf19</i>	This study
pEX18Gm- <i>orf20</i> -UD	Gene replacement vector for <i>orf20</i>	This study
pEX18Gm- <i>orf21</i> -UD	Gene replacement vector for <i>orf21</i>	This study
pEX18Gm- <i>orf17–21</i> -UD	Gene replacement vector for <i>orf17–21</i>	This study
pEX18Gm- <i>orf26</i> -UD	Gene replacement vector for <i>orf26</i>	This study
pEX18Gm- <i>orf13(paaZ)</i> -UD	Gene replacement vector for <i>orf13(paaZ)</i>	This study
pEX18Gm- <i>ech</i> -UD	Gene replacement vector for <i>ech</i>	This study
pEX18Gm- <i>NodN</i> -UD	Gene replacement vector for <i>NodN</i>	This study
pBBR1MCS-2	Mobilizable broad-host-range cloning vector; Km ^r	[49]
pBBR2- <i>paaZ</i>	<i>EcoRI-Sall</i> fragment containing the <i>paaZ</i> gene of HYS cloned into pBBR1MCS-2	This study
pBBR2- <i>paaZE258Q</i>	The <i>EcoRI-Sall</i> fragment containing the <i>paaZ</i> gene with E258Q site mutation cloned into pBBR1-MCS2	This study
pBBR2- <i>ech</i>	<i>XhoI-HindIII</i> fragment containing the <i>ech</i> gene of HYS cloned into pBBR1MCS-2	This study
pBBR2- <i>echD39A</i>	The <i>XhoI-HindIII</i> fragment containing the <i>ech</i> gene with D39A site mutations cloned into pBBR1-MCS2	This study
pBBR2- <i>echH44A</i>	The <i>XhoI-HindIII</i> fragment containing the <i>ech</i> gene with H44A site mutations cloned into pBBR1-MCS2	This study
pBBR2- <i>echG62A</i>	The <i>XhoI-HindIII</i> fragment containing the <i>ech</i> gene with G62A site mutations cloned into pBBR1-MCS2	This study

^aCm, chloramphenicol; Gm, gentamicin; Km, kanamycin; Sp, spectinomycin; Tp, trimethoprim; MCS, multiple-cloning site.

Table S5. Oligonucleotide primers used in this study

Primer	Sequence (5'-3')^{a,b}	Description
<i>orf13-up-1</i>	<u>GGAATTCA</u> ACCGCAACTTCAACGCCAGCTT	Construction of Δ <i>orf13</i>
<i>orf13-up-2</i>	GCTCTAGACATCGGGTGTCCCTCCGGTTTC	Construction of Δ <i>orf13</i>
<i>orf13-down-1</i>	GCTCTAGATGATCTTGAAGTGCGCCCCAC	Construction of Δ <i>orf13</i>
<i>orf13-down-2</i>	<u>CAAGCTT</u> ACTGCTCAACGCCGTGTCC	Construction of Δ <i>orf13</i>
<i>orf13-M-1</i>	TTGTCGCAGCGCACCCAT	Verification of Δ <i>orf13</i>
<i>orf13-M-2</i>	TGCCTTCAACCCACAAGTGA	Verification of Δ <i>orf13</i>
<i>orf17-up-1</i>	<u>GGAATTC</u> GTGGTCAGCGTGGTGGAGCTTGGGA	Construction of Δ <i>orf17</i>
<i>orf17-up-2</i>	<u>CGAGCTC</u> CATGGTCGTTCTCCATCAGGCGCAG	Construction of Δ <i>orf17</i>
<i>orf17-down-1</i>	<u>CGAGCTC</u> TAAGCCCAAGGAGCAGAAGACGA	Construction of Δ <i>orf17</i>
<i>orf17-down-2</i>	<u>CAAGCTT</u> TCGCCGAGATGCCGAGGAAG	Construction of Δ <i>orf17</i>
<i>orf17-M-1</i>	CACGTCGGCGAAGGTGTATTTAC	Verification of Δ <i>orf17</i>
<i>orf17-M-2</i>	TTCCTGCCACGAGCCTACCC	Verification of Δ <i>orf17</i>
<i>orf18-up-1</i>	<u>GGAATTC</u> CGATTTGCCGTGACCAT	Construction of Δ <i>orf18</i>
<i>orf18-up-2</i>	<u>CGAGCTC</u> GGCAATCAGTTCACCAGG	Construction of Δ <i>orf18</i>
<i>orf18-down-1</i>	<u>CGAGCTC</u> TGAGCGCACATTGCTGCGCCT	Construction of Δ <i>orf18</i>
<i>orf18-down-2</i>	<u>CAAGCTT</u> IGCGGTTGCCGTAGAGCAGGGTGA	Construction of Δ <i>orf18</i>

<i>orf18-M-1</i>	CATCGATACGACCGTTGTACAGA	Verification of $\Delta orf18$
<i>orf18-M-2</i>	GCAACTGGCTGGACTACGC	Verification of $\Delta orf18$
<i>orf19-up-1</i>	GGA <u>AATTC</u> TGGGACGAGTTCTACGAAGTGC	Construction of $\Delta orf19$
<i>orf19-up-2</i>	<u>CGAGCTCC</u> AGGTAGGGGATCAGGTC	Construction of $\Delta orf19$
<i>orf19-down-1</i>	<u>CGAGCTCCCC</u> GATGCAACCTGGTGAAGTATT	Construction of $\Delta orf19$
<i>orf19-down-2</i>	CA <u>AGCTT</u> ACTGGCTGAGCAATTCGGTATGGC	Construction of $\Delta orf19$
<i>orf19-M-1</i>	CGACACCGCATCACGGGTTTCAT	Verification of $\Delta orf19$
<i>orf19-M-2</i>	CGCTTCATCGACCAAACCATC	Verification of $\Delta orf19$
<i>orf20-up-1</i>	GGA <u>AATTC</u> GCCAGGGCTACGAAATGCTCC	Construction of $\Delta orf20$
<i>orf20-up-2</i>	<u>CGGATCCC</u> ATGGCGGGCTCTCCGGTCA	Construction of $\Delta orf20$
<i>orf20-down-1</i>	<u>CGGATCCGGG</u> CATATGTAACATGACCCAG	Construction of $\Delta orf20$
<i>orf20-down-2</i>	CA <u>AGCTT</u> AGCGGCGCAAATGGTAGGTGA	Construction of $\Delta orf20$
<i>orf20-M-1</i>	GGCGGCTGTCCAGGTAGAA	Verification of $\Delta orf20$
<i>orf20-M-2</i>	ACAACGGCAAGGCCAAGTA	Verification of $\Delta orf20$
<i>orf21-up-1</i>	GGA <u>AATTC</u> GGTCGAGGAACAGCTGCTTAA	Construction of $\Delta orf21$
<i>orf21-up-2</i>	<u>CGAGCTCC</u> AGTTGTGCGTACATGGTG	Construction of $\Delta orf21$
<i>orf21-down-1</i>	<u>CGAGCTCT</u> GACCGGAGAGCCCGCCATGT	Construction of $\Delta orf21$
<i>orf21-down-2</i>	CA <u>AGCTT</u> CAGCAGGTTGCGGTAGTCG	Construction of $\Delta orf21$
<i>orf21-M-1</i>	ATGGTAGGTGACCTCTTTCAACGC	Verification of $\Delta orf21$
<i>orf21-M-2</i>	GCCCTGCCGATGATCCGCTAT	Verification of $\Delta orf21$

<i>orf17-21-up-1</i>	<u>GGAATTC</u> TGATCCGCTATCGCACCC	Construction of Δ <i>orf17-21</i>
<i>orf17-21-up-2</i>	CGAGCTCCAGTTGTGCGTACATGGT	Construction of Δ <i>orf17-21</i>
<i>orf17-21-down-1</i>	CGAGCTCTAAGCCCAAGGAGCAGAAGACGA	Construction of Δ <i>orf17-21</i>
<i>orf17-21-down-2</i>	CAAGCTTTCGCCGAGATGCCGAGGAAG	Construction of Δ <i>orf17-21</i>
<i>orf17-21-M-1</i>	CGGCGAAGGTGTATTTAC	Verification of Δ <i>orf17-21</i>
<i>orf17-21-M-2</i>	GTCTGGGAGGACCATTCT	Verification of Δ <i>orf17-21</i>
<i>orf26-up-1</i>	<u>GGAATTC</u> GCTGCCGTCAATGGCTACGC	Construction of Δ <i>orf26</i>
<i>orf26-up-2</i>	CGGATCCCATGGTATCTGCCTTTGGTTGC	Construction of Δ <i>orf26</i>
<i>orf26-down-1</i>	CGGATCCTGAGCATGACTGCCCTCAGTC	Construction of Δ <i>orf26</i>
<i>orf26-down-2</i>	CTCTAGAGGCGGTGTCCTTGATGCACTCGG	Construction of Δ <i>orf26</i>
<i>orf26-M-1</i>	CAGCATTGGCGCCGTGGT	Verification of Δ <i>orf26</i>
<i>orf26-M-2</i>	GCGTCGAATACCGAACAGGTCAC	Verification of Δ <i>orf26</i>
RT- <i>rpoB-1</i>	CGGGAGCGACCAAAGATCAG	Real-time qPCR
RT- <i>rpoB-2</i>	CGTACTCCAGGGCAGCATTG	Real-time qPCR
RT- <i>orf13-1</i>	TGAGCGAACGCAAGGAGCA	Real-time qPCR
RT- <i>orf13-2</i>	TATGGCTGCCGACGAACGA	Real-time qPCR
RT- <i>orf17-1</i>	GAACAACCTCGAAATGAATCCGT	Real-time qPCR
RT- <i>orf17-2</i>	AAGACCTGAAGAACCCTACC	Real-time qPCR
RT- <i>orf18-1</i>	TGGCGTGACAAAGCCTGCGTCCTCC	Real-time qPCR
RT- <i>orf18-2</i>	GCGTGGTGGAGCTTGGGATCGTTCCG	Real-time qPCR

RT-<i>orf19-1</i>	CCCGAGCGGCGCAAATGG	Real-time qPCR
RT-<i>orf19-2</i>	CGCAACTGGCTGGACTACG	Real-time qPCR
RT-<i>orf20-1</i>	CAGCGGCTCTTTCTCGTC	Real-time qPCR
RT-<i>orf20-2</i>	ACCCTGTTTGAAGTATTCGTGC	Real-time qPCR
RT-<i>orf21-1</i>	GGTCAGGAGCATTTCGTAGCCC	Real-time qPCR
RT-<i>orf21-2</i>	GCACAACGGCAAGGCCAAGTAC	Real-time qPCR
RT-<i>orf26-1</i>	GTTGACGGCACAGATGACC	Real-time qPCR
RT-<i>orf26-2</i>	CTGTTGCTGACCGCCGAAG	Real-time qPCR
<i>orf13-orf14-RT-1</i>	CGCTCCTCGTGGCTGTA	Reverse transcription PCR
<i>orf13-orf14-RT-2</i>	CGCCTTTCCGTTTCTCAA	Reverse transcription PCR
<i>orf14-orf15-RT-1</i>	CCAGTTTAGCCGTGAAGC	Reverse transcription PCR
<i>orf14-orf15-RT-2</i>	CCTTGCCACCTTAGGGATT	Reverse transcription PCR
<i>orf15-orf17-RT-1</i>	CGAGATGCCGAGGAAG	Reverse transcription PCR
<i>orf15-orf17-RT-2</i>	CGTGCCAGAGCTATCCA	Reverse transcription PCR
<i>orf17-orf18-RT-1</i>	CATCGTTGGCAAAGGC	Reverse transcription PCR
<i>orf17-orf18-RT-2</i>	GGAGGACGCAGGCTTT	Reverse transcription PCR
<i>orf18-orf21-RT-1</i>	AAGCCTGCGTCCTCCA	Reverse transcription PCR
<i>orf18-orf21-RT-2</i>	CTTCATCGACCAAACCATC	Reverse transcription PCR
<i>orf21-orf22-RT-1</i>	CGGGCATCCAGTTCTT	Reverse transcription PCR
<i>orf21-orf22-RT-2</i>	ATCCGCTATCGCACCC	Reverse transcription PCR

<i>orf26-orf27</i> RT-1	CAGCGGGTTGTAGTAGCG	Reverse transcription PCR
<i>orf26-orf27</i> RT-2	GCCTGGTCAGCGAAATCAC	Reverse transcription PCR
<i>orf13-1</i>	GCGTCGACAAACCGGAGGACACCC	<i>orf13</i> amplicon
<i>orf13-2</i>	CGGAATTCTCAAGATCAGGTTGCCACG	<i>orf13</i> amplicon
(<i>orf13</i>) <i>paaZ</i> -E258Q-1	AGCGAGTCGGCTTGGGCGCTGAAGG	<i>paaZ</i> E258Q
(<i>orf13</i>) <i>paaZ</i> - E258Q-2	CCCTTCAGCGCCCAAGCCGACTCGC	<i>paaZ</i> E258Q
<i>ech</i> -up-1	CGGAATTCTGTCGTTCCGGCTCGTT	Construction of Δech
<i>ech</i> -up-2	GGCTGACACCTGGGTCATCACTTGTTTTTCCT	Construction of Δech
<i>ech</i> -down-1	CCCAGGTGTCAGCCCGCCACCCAT	Construction of Δech
<i>ech</i> -down-2	AGGACCGCAGCCTGTGGAACCG	Construction of Δech
<i>ech</i> -up-F	CGGAATTCTGTCGTTCCGGCTCGTT	Construction of Δech
<i>ech</i> -down-R	CCAAGCTTACCGCAGCCTGTGGAACCG	Construction of Δech
<i>ech</i> -M-1	TCGGCCACAGCATGGGCAGCTATAT	Verification of Δech
<i>ech</i> -M-2	CGCCATGACTTGAGCGATGAAGCCA	Verification of Δech
<i>NodN</i> -up-1	AGCGACATACATAGGGCATTGTGACTCTC	Construction of $\Delta NodN$
<i>NodN</i> -up-2	CTCCTGGTTGTCTTGACGGG	Construction of $\Delta NodN$
<i>NodN</i> -down-1	CCGTTGTACTGGTCGTCCTTGA	Construction of $\Delta NodN$
<i>NodN</i> -down-2	CTATGTATGTCGCTCTGCTTCGTCTGA	Construction of $\Delta NodN$
<i>NodN</i> -up-R	CGGAATTCTCCTGGTTGTCTTGACGGG	Construction of $\Delta NodN$
<i>NodN</i> -down-F	CCAAGCTTCCGTTGTACTGGTCGT	Construction of $\Delta NodN$

<i>NodN-M-1</i>	TTCCAGGCGATTGTCATGAAAAGCG	Verification of $\Delta NodN$
<i>NodN-M-2</i>	CACCAGTTGATAGGCACCCAGGGTA	Verification of $\Delta NodN$
RT-ech-1	CCGAGTTCGCCGCCAAGAG	Real-time qPCR
RT-ech -2	GCTCGTCGTTCTGATTGAACAC	Real-time qPCR
<i>ech-1</i>	CGGAATTCAGAAGGAAAAACAAGTGATGACCCA	<i>ech</i> amplicon
<i>ech-2</i>	CCAAGCTTTCAGCCGATGGTGATGGGTGGCGGG	<i>ech</i> amplicon
<i>ech-D39A—1</i>	ATCCAGGTGCACCGGGTTGTGGGCA	<i>echD39A</i>
<i>ech-D39A—2</i>	TGCCCACAACCCGGTGCACCTGGAT	<i>echD39A</i>
<i>ech-H44A—1</i>	ATCCAGGGCCACCGGGTTGTGGTCA	<i>echH44A</i>
<i>ech-H44A—2</i>	TGACCACAACCCGGTGGCCCTGGAT	<i>echH44A</i>
<i>ech-G62A—1</i>	AACATGGCGTGGGCGATACGCTCCT	<i>echG62A</i>
<i>ech-G62A—2</i>	AGGAGCGTATCGCCACGCCATGTT	<i>echG62A</i>

^aUnderline sequences are restriction enzyme sites.

^b Bold sequences refers to bases of the mutant amino acid site.